AAS 11-086

IMPROVED STAR TRACKER INSTRUMENT MAGNITUDE PREDICTION FROM ICESAT FLIGHT TELEMETRY

Noah Smith,[*] Richard Fowell,[†] Sungkoo Bae,[‡] and Bob Schutz[§]

Accurate prediction of instrument magnitudes for both candidate guide stars and potentially interfering near neighbor stars can be difficult because standard astronomical data are not measured at the star tracker spectral passband or angular resolution. Publicly available flight data from the three ICESat star trackers were used to evaluate empirical models for predicting instrument magnitudes and to study prediction errors for near-neighbor and variable stars. Sixty models for predicting instrument magnitudes were evaluated. The test data were CT-602 instrument magnitudes for 4,319 stars. A typical good model had an rms prediction error of 0.071 magnitudes and was applicable to 90% of test stars. The magnitude and color responses of the three trackers and their variation over time were also characterized. Reduced instrument magnitude data is available and summarizes nearly one million star transits of 8,107 ICESat stars with instrument magnitudes less than 7.2 and covering over 90% of the sky. The first release of reduced magnitudes includes 590 stars that do not have instrument magnitudes in the SKY2000 catalog. The flight data is from two Ball CT-602 star trackers and one Goodrich HD-1003 star tracker.

INTRODUCTION

Predicting the apparent brightness or instrument magnitude of stars observed by a star tracker is a critical part of building a flight star catalog. Prediction errors can result in failure to acquire guide stars, star misidentification, and incorrect guide star positions due to near-neighbor effects.[1] Calculating instrument magnitudes has been called "the most delicate step" in constructing a flight star catalog.[2] The astronomical data available for stars is generally taken in different bandwidths, and at a different angular resolution, than that of a typical star tracker.[1-3] Many methods for predicting instrument magnitude have been recommended in the literature.[2-11] Models using flight instrument magnitudes from the SKY2000 catalog performed best. This agreed with a NASA statement that "CT-6xx magnitude observations provide the best data for generating accurate instrumental magnitude predictions for charge-coupled device star trackers or other sensors with similar spectral response characteristics."[11] The results also agreed with a statement that red passband magnitudes have the next best performance, as expected since tracker response typically peaks in the red and infrared passbands.[3]

Star brightness is expressed using a logarithmic magnitude scale. Magnitude m is defined by the ratio of a measured brightness b and a reference brightness b_0.

[*] Doctoral Candidate, Center for Space Research, University of Texas at Austin
[†] Boeing Technical Fellow, Boeing, P.O. Box 92919, MC El Segundo, CA 90009
[‡] Research Scientist/Engineer, Center for Space Research, University of Texas at Austin
[§] Professor and Associate Director, Center for Space Research, University of Texas at Austin

$$m = -2.5\log_{10}\left(b/b_0\right) \tag{1.0}$$

Astronomical magnitudes are measured through color filters or passbands. Standard astronomical passband magnitude types mentioned in this paper are ultraviolet, blue, visual, red, and infrared.[13] Measurements in multiple passbands are used to determine spectral class, which characterizes star color. The standard astronomical spectral classes are O, B, A, F, G, K, M ranging from bluest to reddest. Certain stars are used as references to define magnitudes and spectral classes. For example Vega was used as the reference star for visual magnitudes and the A0 spectral class. For star trackers the magnitude passband is unique to a particular instrument and is commonly called an instrument magnitude. The reference star chosen to define a given tracker's instrument magnitudes varies.[14]

Predicting an instrument magnitude for a particular tracker and star is challenging. Magnitudes in star catalogs for the various passbands are incomplete, inconsistent, and often include groups of stars that appear to be single stars at the resolution of a tracker.[1] Stars are often multiple, variable, or both, which increases the difficulty of predicting the apparent brightness at the tracker passband from data in other passbands. A typical approach is to select a set of reference stars, measure their tracker responses, and fit models of the measurements using astronomical data.[2-5,8] This may be done pre-launch using laboratory tracker response and data from astronomical data sets. Some examples of data sets that have been used are the 180 star Gunn and Stryker catalog and the 13-color photometry 1,380 star Johnson and Mitchell catalog.[2,4,5] Flight measurements of the reference stars from the tracker or a similar instrument can also be used.[5,6,7] If using a similar instrument, it should be noted that there are noticeable differences in response between nominally identical star trackers.[6,15] The fit models can then be used to predict instrument magnitude for stars outside of the reference set. Different combinations of input parameters are available for each star. The best model for a particular star depends on the input parameters available. Input parameters that have been used include standard astronomical passband magnitudes, flight instrument magnitudes, stellar class, subclass, and luminosity. The predictions of empirical models produce significant observed minus predicted outliers. Misidentified stars, multiple stars, variable stars, and atypical stars such as high metallicity stars are problems.

A brief review of the literature on instrument magnitude models is given here. Manon suggests that a color index be calculated from the spectral type and luminosity class and a first or second order polynomial be fitted to differences of astronomical passband magnitudes.[2] Differences of visual and infrared passband magnitudes were used for the French SED12 star tracker.[2] Sande et al. suggests using the most favorable available astronomical magnitude together with a color correction calculated from the Morgan-Keenan stellar class, subclass, and luminosity.[3] For the Ball CT-601 star tracker the astronomical magnitudes are ranked in descending order as: red, visual, photovisual, infrared, blue, photographic, and ultraviolet.[3] Davenport suggests a quadratic fit to the astronomical ultraviolet, blue, and visual magnitudes.[8] Singh et al. used a linear fit in the SKY2000 passband 1 and passband 2 magnitudes.[4] These correspond to astronomical red and infrared magnitude. A quadratic fit to blue and visual magnitudes was used for stars lacking this SKY2000 data.[4] Strunz et al. used a fourth order polynomial fit to blue and visual magnitudes and noted that the fit quality degraded for red stars.[5] Barry et al. used a second order polynomial in blue and visual magnitudes for flight data from two Ball CT-631 trackers.[6] They noted that the fit was poor for blue stars, there was a mean difference of 0.236 magnitudes between the trackers, and the difference varied with star color by up to 0.14 magnitudes.[6] Schmidt et al. gave a computed curve of the offset between instrument magnitudes from an active pixel star tracker and the Hipparcos mission instrument magnitudes.[9]

The NASA ICESat mission was launched on January 13, 2003 into a near-circular, frozen orbit with an altitude of approximately 600 km and an inclination of 94°. The science instrument is the Geoscience Laser Altimeter System (GLAS). ICESat carries four star trackers. The Instrument Star Tracker (IST) is a Raytheon Optical Systems, now Goodrich, HD-1003. It has an 8°×8° field of view, instrument magnitude 6.2 sensitivity, a 512×512 pixel CCD, and tracks up to 6 stars with 10 Hz sampling. The IST tracks any

available stars in the field of view. The Laser Reference Sensor (LRS) is a second, modified 10 Hz HD-1003 with third-party optics and baffle reducing the field of view to 0.5°×0.5° and increasing the sensitivity to instrument magnitude 7.5. LRS data is not discussed further in this paper. GLAS also includes hemispherical resonating gyros sampled at 10 Hz. The two Ball Star Trackers (BST1 and BST2) are 10 Hz Ball CT-602 trackers pointing 30° to either side of the IST. The BSTs have an 8°×8° field of view, instrument magnitude 7.1 sensitivity, a 512×512 pixel CCD, and can track 5 stars simultaneously. The BSTs use position predicts from the flight computer to acquire stars specified in a mission catalog.[16] NASA makes over 570 days of ICESat flight telemetry available online at the National Snow and Ice Data Center.[12] This data set is useful for many attitude determination and attitude sensor studies.[14]

ICESAT, RXTE, AND SKY2000 INSTRUMENT MAGNITUDES

Instrument magnitudes from flight data are included in the SKY2000 catalog as passband 3 magnitudes.[18] The RXTE mission published results for 15,084 instrument magnitudes from the RXTE CT-601 star trackers in the early 2000s.[19] The RXTE magnitudes were included in SKY2000 Version 5 as passband 3 magnitude data.

The first release of ICESat instrument magnitudes accompanies this paper. It includes instrument magnitudes for 590 new stars that did not have RXTE or SKY2000 instrument magnitudes. There are magnitudes from at least one tracker for 6,317 stars. This is about 78% of the 8,107 stars studied for this paper. 2,090 of these stars have magnitudes from all three trackers. Selection criteria included sample sizes, observed minus predicted position residuals, and magnitude measurement variations. The same selection criteria were used for all three trackers. This led to an interesting result. The IST observed more stars than the BSTs because it was not in directed field of view mode, but fewer IST than BST magnitudes met the selection criteria. The release consists of three text files, one for each tracker. The files have the same formatting as the RXTE file. They contain one line for each star. Each line contains a magnitude mean and standard deviation. If the star is classified as variable a magnitude maximum and minimum are also included.

Table 1 summarizes the first release. The first row shows the total number of ICESat stars in each file. The second row gives the number of stars in a file that also appear in the RXTE file and the ratio of this number to the total. Approximately 85% of the ICESat stars are also in the RXTE file. The third row shows the estimated mean and standard deviation of the mean magnitude differences between ICESat and RXTE. These biases are approximately constant over the range of magnitudes. They are probably a result of using a different reference star to calibrate RXTE. ICESat star magnitudes were evaluated by subtracting the magnitude bias and RXTE magnitudes. Stars with magnitude differences larger than three times the sample standard deviation were classified as outliers. The fourth row shows the number of outliers and the ratio of this number to the total.

Table 1. Summary of the first release of ICESat reduced instrument magnitudes.

	IST	BST1	BST2
ICESat stars	3827	4319	4395
Also RXTE stars	3285 (0.858)	3658 (0.847)	3683 (0.838)
Also SKY2000 passband 3 stars	3528 (0.922)	3907 (0.905)	3934 (0.895)
New ICESat only stars	299 (0.078)	412 (0.095)	461 (0.105)
ICESat to RXTE mean bias	0.548 ± 0.002	0.544 ± 0.001	0.619 ± 0.001
ICESat magnitude outliers	32 (0.008)	35 (0.008)	27 (0.006)

As examples of the outliers in the ICESat files, Table 2 describes seven outlier stars that appear in all three files. Pairs of magnitude differences are given for each star and tracker. The first number in each pair is the difference from the RXTE magnitude. The second number is the difference from the magnitude predicted using the results of this paper. In all cases the RXTE magnitudes and predicted magnitudes were similar. For each star the numbers are roughly the same indicating agreement of the three ICESat magnitudes. Henry Draper (HD) identifiers are given for use with astronomical databases.

Table 2. Outlier stars appearing in all three files. The first number in each pair is the difference from the RXTE magnitude. The second is the difference from the magnitude predicted using the results of this paper.

SKYMAP	HD	IST	BST1	BST2	Notes
510044	4817	+0.324, +0.248	+0.255, +0.213	+0.246, +0.209	variable, multiple
3470095	23878	-0.399, -0.242	-0.431, -0.424	-0.388, -0.404	variable
3550050	24534	-0.333, -0.198	-0.299, -0.326	-0.233, -0.296	variable, binary
4030090	25676	-0.325, -0.262	-0.495, -0.486	-0.469, -0.474	variable
15380095	139461	-0.854, -0.660	-0.820, -0.812	-0.854, -0.862	binary
16310033	149009	-1.707, -1.599	-1.757, -2.063	-1.802, -1.261	variable
21560069	208527	+0.319, +0.263	+0.246, +0.208	+0.348, +0.303	variable

Figure 1 below shows the star 15380095 from Table 2 and its binary companion 15380094. The pair has a separation of 11.9 arcseconds, a magnitude difference of 0.1, and both have records in the SKY2000 catalog. At various times the attitude processor identified both members. The ICESat instrument magnitudes for both stars were significantly brighter than predicted due to the near-neighbor.

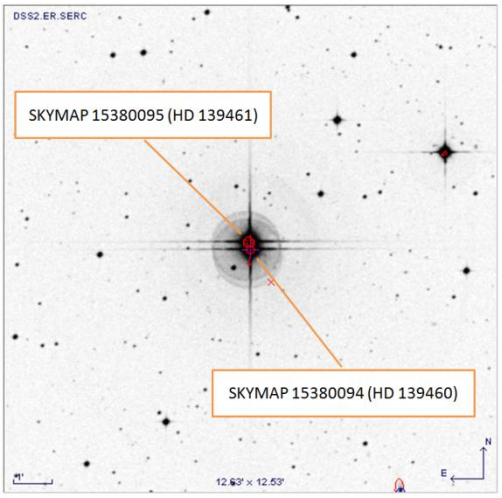

Figure 1. The binary star pair that includes the star 15380095 from Table 2.

Following releases of ICESat instrument magnitudes will include more stars. They will also increase the total number of stars with flight instrument magnitudes by introducing additional stars not previously covered by RXTE or SKY2000.

SUMMARY OF INFORMATION IN SKY2000 FOR THE ICESAT STARS

This section describes the availability of various types of SKY2000 magnitude and spectral information for the ICESat stars. It also describes the frequency of information concerning variability, multiplicity, and bright near-neighbors. The SKY2000 catalog contains records for 299,460 stars. The run-time catalog used here for processing ICESat data consisted of the 45,394 SKY2000 stars with visual magnitudes less than eight. This paper concerns 8,107 identified ICESat stars with instrument magnitudes less than 7.2. Figure 2 below shows the abundances of SKY2000 and ICESat stars versus magnitude. The number of stars increases exponentially with magnitude. The rapid drop-off of ICESat star counts occurs at the magnitude limit of the trackers. In the future the instrument magnitude models and tracker response curves evaluated in this paper will be used to create run-time catalogs based on predicted instrument magnitudes rather than visual magnitudes. This will remove a large group of stars that are too dim to detect. It will also introduce a small group of detectable red stars with visual magnitudes greater than eight. The discussion of tracker response curves below shows that for red stars with spectral class M instrument magnitudes can be up to two magnitudes smaller than visual magnitudes.

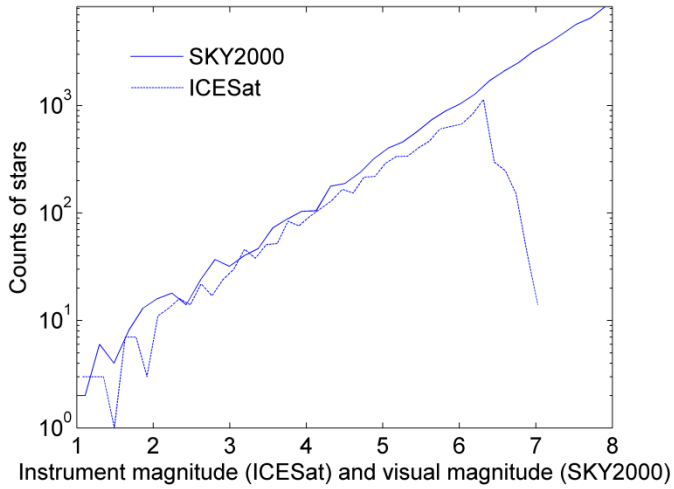

Figure 2. Abundances of SKY2000 stars with visual magnitudes less than eight and ICESat stars.

SKY2000 includes information on astronomical ultraviolet, blue, and visual magnitudes. It also includes information on additional magnitudes defined as passband 1, passband 2, and passband 3. Passband 1 and 2 magnitudes are effectively astronomical red and infrared magnitudes. Passband 3 magnitudes are instrument magnitudes, mostly from the RXTE mission CT-601 star trackers. Table 3 shows the counts of ICESat stars for which the catalog has particular magnitude types. The ratios of the counts to the numbers of ICESat stars are shown in parentheses. The counts are classified by star brightness into five columns with brighter stars to the left and dimmer stars to the right. The table shows that SKY2000 provides complete information for visual magnitudes and nearly complete information for blue magnitudes. Passband 1 and 2 information is above 89% for bright stars. Passband 3 availability is above 86% for all but the dimmest stars.

Table 3. Availability of magnitudes for the ICESat stars, grouped by visual magnitude.

Magnitude type	visual < 4	4 < visual < 5	5 < visual < 6	6 < visual < 7	7 < visual < 8
Ultraviolet	8 (0.016)	26 (0.017)	31 (0.012)	176 (0.058)	138 (0.203)
Blue	487 (0.994)	1508 (0.996)	2875 (0.999)	3035 (0.999)	678 (0.998)
Visual	490 (1.000)	1514 (1.000)	2877 (1.000)	3037 (1.000)	679 (1.000)

Passband 1	466 (0.951)	1398 (0.923)	1865 (0.648)	1874 (0.617)	172 (0.253)
Passband 2	461 (0.941)	1356 (0.896)	587 (0.204)	230 (0.076)	16 (0.024)
Passband 3	465 (0.949)	1414 (0.934)	2638 (0.917)	2632 (0.866)	462 (0.680)

Table 4 shows the availability and frequency of additional information for the ICESat stars. Spectral class represents a range from bluer stars to redder stars. Luminosity class represents a range from supergiant stars to dwarf stars. Spectral class and luminosity class were converted to integers for use as input variables to instrument magnitude models. Variable stars were defined here as those whose catalog records included values for variability maximum and minimum magnitudes. A better definition for future use may be stars with a non-empty variable name field. This field gives a text variable star name for known variables and a numeric identifier for suspected variables. Bright neighbor stars had records that included an angular separation to a bright near-neighbor. SKY2000 defines a bright near-neighbor as having an angular separation of up to 0.6 degrees and a magnitude difference less than two. 0.6 degrees is a large separation for the ICESat trackers so more restricted criteria for bright near-neighbors are used in practice, but the frequencies shown here are rough indicators. Blended position and blended visual magnitude stars had SKY2000 records that were calculated by combining more than one star. Both indicate cases where a near-neighbor has a significant effect on measurements.

Table 4. Availability and frequency of additional information for the ICESat stars, grouped by visual magnitude.

Information type	visual < 4	4 < visual < 5	5 < visual < 6	6 < visual < 7	7 < visual < 8
Spectral class	486 (0.992)	1506 (0.995)	2860 (0.994)	3026 (0.996)	664 (0.978)
Luminosity class	489 (0.998)	1491 (0.985)	2672 (0.929)	2485 (0.818)	496 (0.731)
Variable	294 (0.600)	742 (0.490)	781 (0.271)	535 (0.176)	130 (0.192)
Multiple	271 (0.553)	702 (0.464)	855 (0.297)	637 (0.210)	133 (0.196)
Bright neighbor	82 (0.167)	437 (0.289)	1736 (0.603)	2485 (0.818)	666 (0.981)
Blended position	46 (0.094)	96 (0.063)	45 (0.016)	35 (0.012)	17 (0.025)
Blended visual	19 (0.039)	53 (0.035)	69 (0.024)	23 (0.008)	6 (0.009)

The SKY2000 specification document has further details on available information.[18] Additional types of star identifiers for linking SKY2000 records to records in other star catalogs are of special interest. In particular, the Henry Draper identifiers in SKY2000 can be compared to the HD identifiers contained in the Hipparcos Main Catalog to link SKY2000 identifiers to Hipparcos identifiers for 82% of the 45,394 SKY2000 stars with visual magnitudes up to eight.

TRACKER RESPONSE TO BRIGHTNESS AND COLOR

Brightness and color can be characterized using a variety of quantities. Here visual magnitude was used for brightness and spectral class was used for color. Tracker response was defined as the differences between instrument magnitudes and visual magnitudes. Figure 3 shows a typical scatter plot of tracker responses versus visual magnitudes for several thousand stars. Points higher in the plot have dimmer instrument magnitudes and lower responses. Points lower in the plot have brighter instrument magnitudes and high responses. There is vertical banding of the points by spectral class with blue stars in higher bands and red stars in lower bands. This is caused by the greater sensitivity of the detector to red light. The increased scatter for dim stars may be due to thresholding by the tracker.[20]

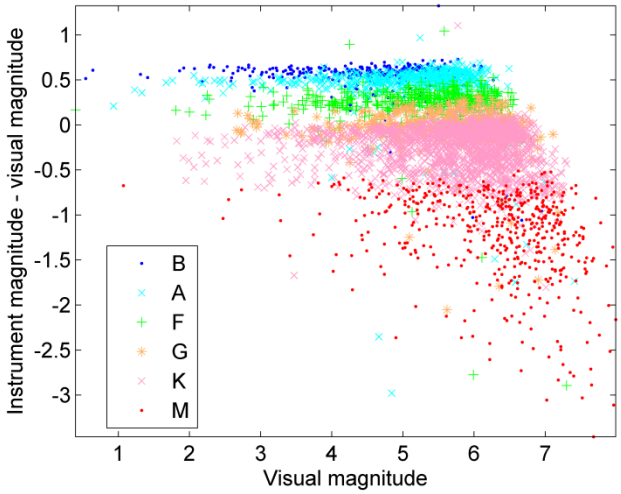

Figure 3. Typical tracker response to visual magnitude and spectral class.

The responses of multiple trackers could be compared by superimposed or side-by-side scatter plots. A different method was used here. For each tracker, six curves were fit to the bands of scatter plot points for the six spectral classes. Between visual magnitudes three and six the bands of scatter plot points were roughly linear so linear fits in this region were used. The responses of multiple trackers were compared by superimposing their fit lines, rather than their scatter plots. Figure 4 below compares the fit lines for the ICESat and RXTE trackers. The responses of the three ICESat trackers to brightness and color are similar but have statistically significant differences. The response of the RXTE tracker shows the bias from the ICESat responses described previously in Table 1.

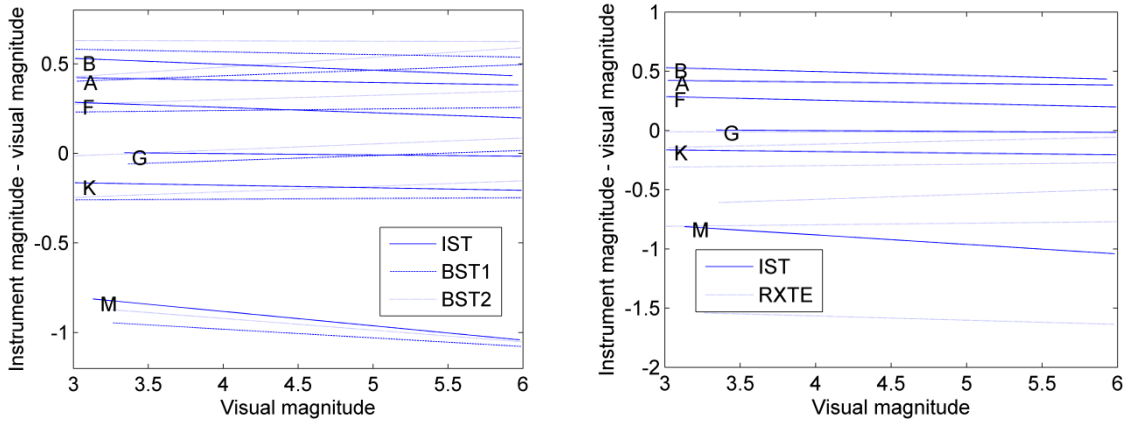

Figure 4. Linear fits of the various tracker responses to visual magnitude and spectral class.

COMPARISON OF MAGNITUDE PREDICTION MODELS

Sixty models were compared using the 4,319 BST1 stars in the first release of ICESat instrument magnitudes. Visual, blue, passband 1, passband 2, and passband 3 magnitudes were used as model inputs. Passband 3 magnitudes were expected to perform best as they are flight instrument magnitudes from RXTE and SKY2000. Passband 1 and 2 magnitudes were expected to perform next best. They correspond to astronomical red and infrared magnitudes where star tracker response is strongest. Models with and

without a color term were evaluated. The color term was an integer *s* representing star spectral class. A model without a color term

$$m_i = c_0 + c_1 m_v + c_2 m_b \tag{1.1}$$

had the following form with a color term.

$$m_i = c_0 + c_1 s + c_2 m_v + c_3 m_b \tag{1.2}$$

The information contained in the color term was mostly redundant if multiple passband magnitudes were included in the model since the difference of two passband magnitudes indicates color. Table 5 shows the performance of the various models. Magnitude prediction error was defined as the difference of an observed and predicted magnitude. Prediction errors were calculated for every test star and the RMS errors are shown in the table along with the ratio of test stars available for use in the model.

Table 5. RMS magnitude prediction errors for various models and 4,319 BST1 test stars. The relative number of stars available for a particular model is shown in parentheses. The model inputs were visual magnitude (V), blue magnitude (B), passband 1 magnitude (1), passband 2 magnitude (2), and passband 3 magnitude (3).

Model inputs	Linear model	Quadratic model	Linear with color	Quadratic with color
V	0.543 (1.000)	0.511 (1.000)	0.370 (0.998)	0.355 (0.998)
B	0.762 (0.997)	0.725 (0.997)	0.460 (0.995)	0.425 (0.995)
1	0.152 (0.702)	0.152 (0.702)	0.149 (0.702)	0.149 (0.702)
2	0.387 (0.303)	0.387 (0.303)	0.242 (0.303)	0.239 (0.303)
3	0.071 (0.905)	0.071 (0.905)	0.071 (0.903)	0.071 (0.903)
V, B	0.361 (0.997)	0.342 (0.997)	0.349 (0.995)	0.323 (0.995)
V, 1	0.152 (0.702)	0.130 (0.702)	0.148 (0.702)	0.130 (0.702)
V, 2	0.136 (0.303)	0.134 (0.303)	0.136 (0.303)	0.134 (0.303)
V, 3	0.071 (0.905)	0.071 (0.905)	0.069 (0.903)	0.069 (0.903)
B, 1	0.150 (0.700)	0.133 (0.700)	0.148 (0.700)	0.132 (0.700)
B, 2	0.156 (0.301)	0.153 (0.301)	0.153 (0.301)	0.151 (0.301)
B, 3	0.071 (0.901)	0.070 (0.901)	0.070 (0.900)	0.070 (0.900)
1, 2	0.139 (0.302)	0.138 (0.302)	0.136 (0.302)	0.136 (0.302)
1, 3	0.069 (0.648)	0.061 (0.648)	0.068 (0.648)	0.061 (0.648)
2, 3	0.049 (0.284)	0.045 (0.284)	0.048 (0.284)	0.045 (0.284)

Passband 3 magnitudes perform the best as expected. They do contain a constant bias from the ICESat magnitudes because they are mostly RXTE flight instrument magnitudes. Passband 1 magnitudes perform next best but are available for fewer ICESat stars.

MAGNITUDE PREDICTION ERRORS

Prediction errors can be grouped by tracker, visual magnitude, and spectral class. Table 6 is an example. The predictions used a linear model with passband 3 magnitude as input. The number of test stars is shown in parentheses. The prediction errors for RXTE are zero because passband 3 magnitudes are in fact RXTE observed magnitudes.

Table 6. RMS prediction errors grouped by tracker, visual magnitude, and spectral class. The number of test stars is shown in parentheses.

Spectral class	Tracker	visual < 4	4 < visual < 5	5 < visual < 6	6 < visual < 7	7 < visual < 8
B	IST	0.049 (70)	0.058 (96)	0.065 (214)	0.160 (9)	-- (0)
	BST1	0.049 (83)	0.049 (124)	0.081 (139)	0.111 (9)	-- (0)
	BST2	0.037 (84)	0.053 (132)	0.061 (153)	0.126 (5)	-- (0)
	RXTE	0.000 (78)	0.000 (116)	0.000 (137)	0.000 (7)	-- (0)
A	IST	0.031 (54)	0.038 (119)	0.067 (319)	0.081 (25)	0.032 (3)
	BST1	0.029 (66)	0.037 (141)	0.063 (311)	0.055 (42)	0.024 (1)
	BST2	0.031 (70)	0.041 (146)	0.066 (275)	0.079 (48)	0.064 (1)
	RXTE	0.000 (60)	0.000 (128)	0.000 (288)	0.000 (34)	0.000 (1)
F	IST	0.045 (32)	0.046 (79)	0.065 (201)	0.172 (56)	0.012 (1)
	BST1	0.047 (44)	0.041 (89)	0.076 (205)	0.149 (74)	0.027 (1)
	BST2	0.037 (47)	0.043 (87)	0.075 (200)	0.151 (93)	0.032 (1)
	RXTE	0.000 (41)	0.000 (82)	0.000 (194)	0.000 (63)	0.000 (1)
G	IST	0.061 (21)	0.046 (58)	0.054 (161)	0.085 (133)	0.097 (2)
	BST1	0.063 (21)	0.033 (71)	0.041 (179)	0.069 (156)	0.066 (4)
	BST2	0.057 (24)	0.036 (64)	0.054 (180)	0.075 (167)	0.103 (2)
	RXTE	0.000 (18)	0.000 (63)	0.000 (163)	0.000 (146)	0.000 (1)
K	IST	0.038 (74)	0.034 (155)	0.090 (540)	0.074 (654)	0.121 (9)
	BST1	0.034 (100)	0.028 (211)	0.082 (602)	0.060 (696)	0.063 (35)
	BST2	0.038 (102)	0.033 (215)	0.087 (613)	0.065 (687)	0.073 (33)
	RXTE	0.000 (96)	0.000 (203)	0.000 (564)	0.000 (659)	0.000 (32)
M	IST	0.189 (9)	0.195 (34)	0.057 (82)	0.148 (185)	0.181 (102)
	BST1	0.051 (11)	0.063 (41)	0.048 (103)	0.059 (217)	0.170 (114)
	BST2	0.035 (10)	0.066 (41)	0.048 (107)	0.059 (214)	0.137 (113)
	RXTE	0.000 (11)	0.000 (39)	0.000 (99)	0.000 (211)	0.000 (113)

The numbers of dim stars increases dramatically in the red spectral classes K and M. This demonstrates the higher sensitivity of the trackers to red stars.

Table 7 shows the means and sample standard deviations of the prediction errors for three important models and the first release of ICESat magnitudes. The number of stars is shown in parentheses. For a given tracker each star was included in the table once using the best possible model.

Table 7. Prediction error means and sample standard deviations for three important models and the first ICESat magnitudes release. The model inputs were visual magnitude (V), blue magnitude (B), passband 1 magnitude (1), and passband 3 magnitude (3).

Model inputs	IST	BST1	BST2
1, 3	-0.000 ± 0.072 (2463)	-0.000 ± 0.061 (2800)	-0.000 ± 0.059 (2879)
V, 3	0.000 ± 0.090 (1065)	0.000 ± 0.062 (1107)	0.002 ± 0.064 (1055)
V, B	0.007 ± 0.387 (298)	0.012 ± 0.402 (411)	0.010 ± 0.406 (460)

Negative prediction errors can be caused by near-neighbor stars. The observed magnitude of the identified star is smaller than its predicted value because of light from neighboring stars. Figure 5 shows an example. The IST acquired these stars regularly. They compose the Trapezium open cluster in the Orion Nebula. There are at least five relatively bright stars within 30 arcseconds. At various times the attitude processor identified HD 37022 and HD 37023 and treated them as the guide star. In both cases the magnitude prediction errors were high due to the various other light sources.

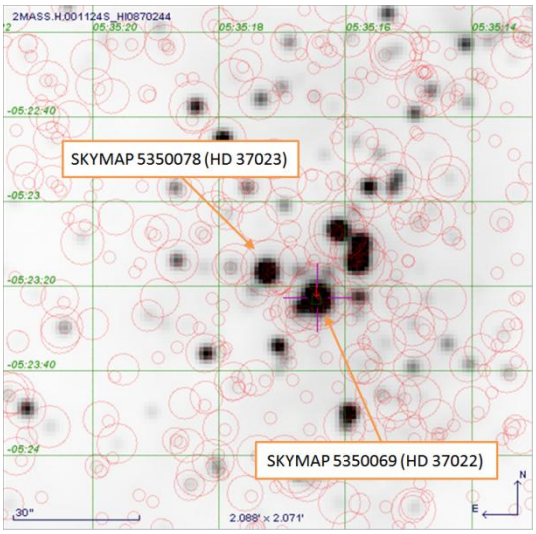

Figure 5. Stars with large magnitude prediction errors that were acquired regularly by the IST. They compose the Trapezium open cluster in the Orion Nebula. Image generated by SIMBAD internet database.

For a sample of large prediction errors, Table 8 shows stars whose errors were large for both BSTs. Passband 3 magnitudes and models were available for all of these stars. Smithsonian Astrophysical Observatory (SAO) identifiers are given for use with astronomical databases. The first two stars in the table are the members of the binary pair shown above in Figure 1. The table demonstrates that there is a wide distribution including both large positive and large negative prediction errors.

Table 8. Stars whose prediction errors were large for both BSTs.

SKYMAP	SAO	BST1 prediction	BST2 prediction	BST1 error	BST2 error	Note
15380094	140671	6.841	6.946	-0.808	-0.905	

15380095	140672	6.809	6.913	-0.775	-0.838	
16310033	84423	5.91	5.907	-0.773	-0.74	
4030090	169080	6.285	6.373	-0.486	-0.473	
13390077	100654	6.322	6.4	-0.386	-0.408	variable
3470095	168836	6.149	6.254	-0.388	-0.375	
3550050	56815	6.671	6.769	-0.345	-0.302	variable
10180019	178644	6.066	6.149	-0.27	-0.269	variable
13550141	258683	5.786	5.852	-0.273	-0.245	
22230017	34387	5.724	5.806	-0.252	-0.259	variable
14130055	29045	5.04	5.033	-0.298	-0.196	
10140	147042	3.516	3.541	-0.243	-0.235	variable
20170002	125646	6.248	6.334	-0.242	-0.23	
13470039	252448	5.146	5.209	-0.231	-0.221	variable
16040068	159665	4.572	4.65	-0.218	-0.221	
10340162	178993	6.516	6.616	-0.208	-0.225	
2020164	110291	4.525	4.589	-0.218	-0.213	
23050063	191638	6.402	6.49	-0.226	-0.192	variable
14560071	206112	5.913	5.997	-0.192	-0.224	
10430073	118448	5.835	5.904	-0.202	-0.201	
10210005	15147	6.155	6.242	0.187	0.187	variable
510044	11430	5.053	5.126	0.191	0.183	variable
16350003	17155	5.614	5.696	0.193	0.19	variable
13490099	224471	3.835	3.852	0.214	0.184	variable
22250055	127520	5.294	5.353	0.201	0.213	variable
15150086	257252	6.548	6.645	0.227	0.193	
16270002	159918	4.475	4.536	0.2	0.237	variable
23560031	192250	6.332	6.419	0.21	0.237	pulsating star
8290136	135976	5.053	5.128	0.29	0.233	variable
22550003	108255	5.974	6.056	0.258	0.276	variable
14010054	120228	6.283	6.369	0.3	0.321	
23000016	35039	4.858	4.879	0.33	0.388	variable
2030178	37735	1.409	1.427	0.398	0.453	binary

Both positive and negative prediction errors can be caused by variable stars. Figure 6 below shows BST2 instrument magnitudes for the Cepheid variable Mekbuda (Zeta Gemini, SKYMAP 7040034, HD 52973). The SKY2000 values for the variability max and min visual magnitudes are 3.62 and 4.18, the

visual magnitude is 4.01, and the period is 10.15 days. The variability amplitude is significantly larger than the prediction uncertainty of about 0.06 for passband 3 models. The prediction error varies periodically with star brightness.

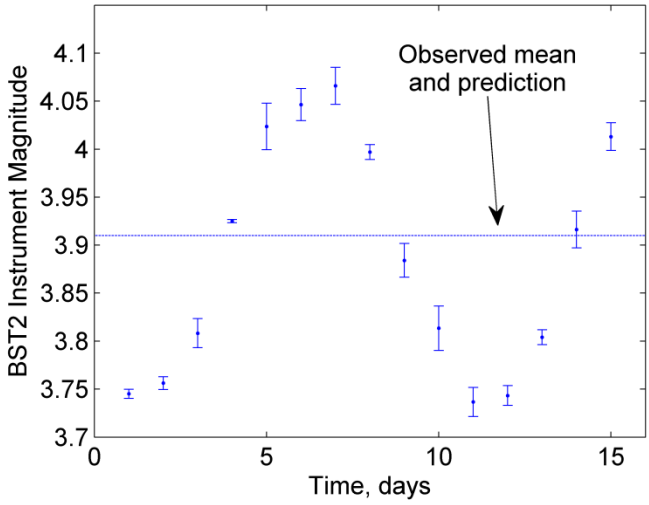

Figure 6. BST2 instrument magnitudes for the Cepheid variable Mekbuda (Zeta Gemini, SKYMAP 7040034, HD 52973).

Table 9 shows variable stars with large prediction errors. The last two columns of the table show the variability amplitude and period information from SKY2000. Henry Draper (HD) identifiers are given for use with astronomical databases.

Table 9. Variable stars with large prediction errors.

SKYMAP	HD	Prediction	Error	Amplitude	Period (days)
2530146	18242	4.928	1.109	9.6	407.6
23430138	222800	4.186	-0.3	6.6	387
9320044	82901	4.052	1.111	6.6	308.7
19060091	177940	4.553	-0.555	6.5	284.2
21350031	206362	6.09	-0.691	5.5	486.8
13490007	120285	3.185	0.403	3.9	361
7130116	56096	2.901	0.914	3.6	140.6
18380073	172171	4.652	-0.965	3.3	328.9
8290136	71887	5.053	0.29	3.2	290
10070209	88028	5.524	-0.277	2.3	780
16350003	150077	5.614	0.193	2.3	78
22230017	212466	5.806	-0.259	2.1	346
23590013	224583	5.969	-0.562	2	141
6050169	41698	4.645	-0.406	1.6	89

8580035	76734	5.774	-0.689	1.5	60
13470039	119796	5.146	-0.231	1.3	--
8240086	70938	4.936	0.246	1.3	--
18500232	174638	4.021	-0.211	1.1	12.9
6250055	44990	5.978	-0.255	1	27
3550050	24534	6.671	-0.345	1	--
22030149	209598	4.684	-0.227	0.9	929.3
16010041	142941	6.463	-0.282	0.9	6.3
16270002	148184	4.536	0.237	0.8	--
23000016	217476	4.879	0.388	0.8	--
22550003	216724	6.056	0.276	0.7	--
20510095	198726	5.9	0.292	0.7	4.4
23050063	218074	6.402	-0.226	0.7	--
11450105	102159	5.451	-0.254	0.6	42
13490099	120324	3.747	0.248	0.6	--
3260092	21242	6.441	0.319	0.4	6.4
10180019	89353	6.066	-0.27	0.4	--
7520023	64052	4.962	-0.259	0.3	35
22250055	212571	5.353	0.213	0.3	--
15380045	139608	4.547	-0.275	0.3	--
2590085	18482	5.649	-0.197	0.2	--
7260238	58978	6.425	-0.221	0.2	--

Instrument magnitude variations can be caused by variable stars, light from the sun or moon, decreasing tracker sensitivity due to aging, or other instrument errors. Trackers aging can result in changes in sensitivity. Table 10 shows magnitude variations over time for groups of stars. The earliest observations of individual stars were used to define reference values and compared to later observations. Statistics for the tables below were calculated using two orbital revolutions from 228 days in the survey with 457,438 tracker passes of 6,404 unique stars. The number of stars used is indicated in parentheses.

Table 10. Estimated variations of magnitudes over time for groups of stars due to tracker aging.

Time period	IST	BST1	BST2
2003 to 2004	-0.017 ± 0.045 (43)	-0.002 ± 0.046 (111)	-0.016 ± 0.043 (112)
2003 to 2005	0.005 ± 0.032 (46)	0.010 ± 0.032 (42)	0.011 ± 0.030 (53)
2003 to 2006	-0.002 ± 0.040 (56)	-0.016 ± 0.035 (218)	-0.034 ± 0.059 (222)
2003 to 2006	-0.015 ± 0.057 (146)	-0.006 ± 0.028 (176)	0.021 ± 0.023 (169)
2003 to 2007	-0.011 ± 0.031 (38)	0.007 ± 0.021 (52)	0.031 ± 0.028 (47)

For all three trackers the estimated mean changes appear to be zero-mean variations and not significant compared to the uncertainties. Some evidence has been seen for small decreases in sensitivity for individual stars. The question of aging effects will continue to be investigated using more sophisticated methods during ongoing reprocessing.

CONCLUSION

These results agree that flight instrument magnitudes are the best inputs for magnitude prediction. Reduced flight magnitudes from the ICESat data are a useful resource. Magnitude prediction errors due to near-neighbor and variable stars are significant and should be handled systematically.

ACKNOWLEDGEMENTS

This research has made use of the SIMBAD database, operated at CDS, Strasburg, France. It has also made use of the JPL On-Line Solar System Data Service. The ICESat data used are publicly available from the National Snow and Ice Data Center.[21]

REFERENCES

[1] Sande, Christopher B., Natanson, Gregory A., Treadwell, David A., "Effects of Uncataloged Near-Neighbor Stars on CCDST Operation", Flight Mechanics Symposium Goddard Space Flight Center Greenbelt, Maryland.
URL: http://goo.gl/wPfU (Archived by WebCite® at http://www.webcitation.org/5bcnXSzuI)

[2] Manon, F., "Astronomical References for Star Sensors", Chapter 8 of: Carrou, Jean-Pierre, *Spaceflight Dynamics*, Cepadues-Editions , 1995, Vol. 1, pp. 508-558.

[3] Sande, C.B., Brasoveanu, D., Miller, A.C., Home, A.T., Tracewell, D.A., "Improved Instrumental Magnitude Prediction Expected from Version 2 of the NASA SKY2000 Master Star Catalog", AAS 98-362, : AAS/GSFC 13th Intl Symp. on Space Flight Dyn, Volume 2, 741-754,, May 11-15 1998.

[4] Singh, Vandana, Pullaiah, D., Sreenivasa Rao, J., T.H Shashikala, T.H., G. Nagendra Rao, G.,Jain, Y.K. and T.K.Alex, "Generation and Validation of On-board Star Catalog for Resourcesat – I Star Tracker", AIAA 2004-5391, AIAA/AAS Astrodynamics Specialist Conference and Exhibit 16 - 19 August 2004, Providence, Rhode Island

[5] Strunz, Harry C., Baker, Troy, Ethridge, David, "Estimation of stellar instrument magnitudes", Proc. SPIE Vol. 1949, p. 228-235, Sept. 1993.
URL: http://goo.gl/q33s (Archived by WebCite® at http://www.webcitation.org/5t7PXXt2h)

[6] Barry, Karen, Hindman, Mark, Yates, Russell, "Application of Flight Data to Space Shuttle CCD Star Tracker Catalog Design", AAS 93-015.

[7] NM Gomes, M Fouquet and WH Steyn, "Astrolabe - A Low Cost Autonomous Star Camera", 4th International Symposium on Small Satellites Systems and Services, Antibes France, 14-18 September 1998, Proceedings: Session 6/7.,
URL: http://goo.gl/ujzW (Archived by WebCite® at http://www.webcitation.org/5c38t7C6o)

[8] Davenport, Paul B., "The Approximation of Stellar Energy Distributions and Magnitudes from Multi-Color Photometry", NASA TM X-63185, Goddard Space Flight Center, April 1968, 13pp.
URL: http://goo.gl/asQN (Archived by WebCite® at http://www.webcitation.org/5t7PDll70)

[9] Schmidt, U, Michel, KI., Airey, S.P., "Active Pixel Sensor Technology Applied in Autonomous Star Sensors – Advantages and Challenges", AAS 07-063, G&C 2007, February 3-7, 2007, Breckenridge.

[10] R. W. H. Van Bezooijen, L. Degen, H. Nichandros, "Guide Star Catalog for the Spitzer Space Telescope Pointing Calibration and Reference Sensor." SPIE Proceedings Vol. 5487, Optical, Infrared, and Millimeter Space Telescopes, Proceedings of the SPIE, Vol. 5487, pp. 253-265, 2004.
URL: http://goo.gl/NCQd (Archived by WebCite® at http://www.webcitation.org/5t7PRdJA3)

[11] NASA/TM-2004–212747 Flight Dynamics Analysis Branch End of Fiscal Year 2003 Report, C. Gramling et. al., ed., February 2004.

[12] National Snow and Ice Data Center, "ICESat/GLAS Data".
URL: http://goo.gl/air8 (Archived by WebCite® at http://www.webcitation.org/5t7Q7gxPS)

[13] H. L. Johnson, W. W. Morgan, "Fundamental stellar photometry for standards of spectral type on the revised system of the Yerkes spectral atlas." *Astrophysical Journal*. Vol. 117, 1953, pp. 313-352.

[14] R. A. Fowell, N. Smith, S. Bae, B. E. Schutz, "Bad Stars." Paper AAS 09-012, Annual AAS Rocky Mountain Conference, Breckenridge, Colorado, 2009.
URL: http://goo.gl/qR9X (Archived by WebCite® at http://www.webcitation.org/5t9dPNlTO)

[15] Anon. "Delivery documentation for the SKYMAP Aqua Star Catalog". 2002-04-10.
URL: http://goo.gl/tdym (Archived by WebCite® at http://www.webcitation.org/5brwUCF7J)

[16]. Zwally, H.J., R. Schutz, C. Bentley, J. Bufton, T. Herring, J. Minster, J. Spinhirne, and R. Thomas. 2003, updated 2008. GLAS/ICESat L1A Global Laser Pointing Data V028/V029. Boulder, CO, National Snow and Ice Data Center. Digital media.

[17] B. E. Schutz, S. Bae, N. Smith, J. M. Sirota, "Precision Orbit And Attitude Determination For ICESat." Paper AAS 08-305, F. Landis Markley Astronautics Symposium, Cambridge, Maryland, 2008.
URL: http://goo.gl/95IQ (Archived by WebCite® at http://www.webcitation.org/5t9ddSz5f)

[18] C. Sande, N. Ottenstein, D. Tracewell, D. Oza, "SKYMAP Requirements, Functional, and Mathematical Specifications." Report No. CSC-96-932-24, Computer Sciences Corporation Report, CSC-96-932-24, 1999.
URL: (Archived by WebCite® at http://www.webcitation.org/5jrOOwX4o)

[19] Tracewell, David. Flight Dynamics' Star Catalog Database. NASA FDF.
URL: http://goo.gl/O2Qm (Archived by WebCite® at http://www.webcitation.org/5bfVD1j6s)

[20] Kruijff, M., Heide, E.J. v.d. , de Boom, C.W., Heiden, N. v.d., "Star Sensor Algorithm Application and Spin-Off", IAC-03-A.5.03, 2003.
URL: (Archived by WebCite® at http://www.webcitation.org/5brqaea5E)

[21] Zwally, H.J., R. Schutz, C. Bentley, J. Bufton, T. Herring, J. Minster, J. Spinhirne, and R. Thomas. 2003, updated current year. GLAS/ICESat L1A Global Laser Pointing Data V018, 15 October to 18 November 2003. Boulder, CO: National Snow and Ice Data Center. Digital media.